Electron-Induced Neutron Knockout from ^{4}He

A. Misiejuk,[1] Z. Papandreou,[2] E. Voutier,[3] Th. S. Bauer,[4] H. P. Blok,[5] D. J. Boersma,[1] H.W. den Bok,[1] E. E.W. Bruins,[1] F. Farzanpay,[2] K. Grüner,[3] W. H. A. Hesselink,[5] G. M. Huber,[2] E. Jans,[4] N. Kalantar-Nayestanaki,[6] W.-J. Kasdorp,[4] J. Konijn,[4] J.-M. Laget,[7] L. Lapikás,[4] G. J. Lolos,[2] G. J. G. Onderwater,[5] A. Pellegrino,[5] R. Schroevers,[4] C. M. Spaltro,[5] R. Starink,[5] G. van der Steenhoven,[4] J. J. M. Steiger,[4] J. L. Visschers,[4] H.W. Willering,[1] and D. M. Yeomans[1]

[1]*Universiteit Utrecht/NIKHEF, P.O. Box 80000, 3508 TA Utrecht, The Netherlands*
[2]*Department of Physics, University of Regina, Regina, Saskatchewan, S4S 0A2, Canada*
[3]*Institut des Sciences Nucléaires, IN2P3-CNRS/UJF, 53 Avenue des Martyrs, 38026 Grenoble, France*
[4]*NIKHEF, P.O. Box 41822, 1009 DB Amsterdam, The Netherlands*
[5]*Department of Physics and Astronomy, Vrije Universiteit, 1081 HV Amsterdam, The Netherlands*
[6]*KVI, Zernikelaan 25, 9747 AA Groningen, The Netherlands*
[7]*CEA-Saclay, Service de Physique Nucléaire, 91191 Gif-sur-Yvette CEDEX, France*

(Received 31 January 2002; published 3 October 2002)

The differential cross section for electron-induced neutron knockout in the reaction ^{4}He$(e, e'n)^3$He has been measured for the first time with a statistical accuracy of 11%. The experiment was performed in quasielastic kinematics at a momentum transfer of 300 MeV/c and in the missing-momentum range of 25–70 MeV/c. The comparison of the data with theoretical calculations shows an impressive increase of the cross section resulting from final state interaction effects. Specifically , the p-n charge-exchange process dominates the cross section in this kinematical regime.

DOI: 10.1103/PhysRevLett.89.172501 PACS numbers: 13.40.Gp, 14.20.Dh, 25.30.Fj

During the past decades, $A(e, e'N)$ electron-nucleus quasielastic scattering (QES) has provided us with a wealth of data allowing us to study nuclear structure, the role of subnucleonic degrees of freedom in reaction mechanisms, and the electromagnetic form factors of nucleons, among others. Nearly all QES data on nuclei heavier than ^{3}He have been obtained from the proton-knockout reaction in two-spectrometer coincidence experiments [1]. It is desirable to avail of QES data for the neutron-knockout reaction, in particular, for the study of neutron electromagnetic form factors and bound-state wave functions. Before such issues can be addressed, the mechanism of the $(e, e'n)$ reaction needs to be understood.

Within the framework of the plane wave impulse approximation (PWIA), the cross section for this knockout reaction can be factorized into the product of the elementary e-N cross section, a spectral function, and kinematical factors. However, this first-order picture has been proven incomplete (e.g., Refs. [2,3]): additional mechanisms must be considered, such as meson exchange currents (MEC), rescattering or final state interactions (FSI), as well as nuclear-medium modifications of basic particle properties.

Unlike proton knockout, the $(e, e'n)$ channel remains largely unexplored, and no data are available for nuclei with mass $A \geq 4$. The reason for this is that, for momentum transfers of a few hundred MeV/c and small scattering angles, the corresponding coupling of the virtual photon to the neutron is 5 to 10 times weaker than the coupling to the proton. This, compounded with a typical detection efficiency for neutrons of about 10%, makes this channel very difficult to access.

The mechanism of the $(e, e'n)$ reaction was first studied in the pioneering work of Daman [4], in which the recoil technique was used to measure the reaction ^{4}He$(e, e'^3$He$)n$ in the missing-momentum range 175–210 MeV/c. These data confirm qualitatively that quasielastic proton and neutron knockout differ substantially. PWIA, which usually overestimates experimental cross sections in the case of $(e, e'p)$ reactions, falls short by about half an order of magnitude for the case of the ^{4}He$(e, e'^3$He$)n$ reaction. The author, in line with earlier work [5], argues that p-n rescattering is responsible for providing the additional strength in the neutron-knockout channel. This charge-exchange process potentially affects every nucleon-knockout reaction, and thus must be well understood.

In view of the absence of reliable data on e-n QES, the first goal is to establish a precise value for the cross section under quasielastic kinematics and the role played by FSI. This is specifically important at vanishing missing momentum, where in quasielastic electron-proton reactions rescattering processes are relatively less important. This Letter presents an accurate study of the role of multistep processes in the ^{4}He$(e, e'n)$ reaction at small missing momenta. The ^{4}He target was chosen for a number of reasons. First, it has a well-understood structure in which protons and neutrons occupy similar states. Second, its high nuclear density — among few-body systems — is expected to enhance charge-exchange effects. Third, ^{4}He is a nucleus which has been extensively studied experimentally, not only via inclusive electron scattering, but also through quasielastic proton knockout [2,3,6–8]. Particularly, the latter experiments

have shown that the ^{4}He$(e, e'p)$ cross section at small missing momentum is dominated by the one-step quasielastic amplitude.

The ^{4}He$(e, e'n)^3$He experiment was performed at the accelerator complex MEA-AmPS of NIKHEF, Amsterdam, using an electron beam of 586 MeV with an average intensity of 1 μA and a 50% duty cycle. Incident electrons impinged radially on a ^{4}He gas target (at 15 K and 1 MPa) contained in a cylindrical vessel of 5 cm diameter with wall thickness of 0.2 mm Al. The relative target thickness was monitored throughout the experiment by counting single events from the (e, e') reaction in the quadrupole-dipole-dipole magnetic spectrometer [9].

The quadrupole-dipole-quadrupole (QDQ) magnetic spectrometer [10] was used to detect electrons in coincidence with neutrons which were detected in a time-of-flight (TOF) plastic-scintillator detector array. The QDQ — whose acceptance was collimated to subtend a solid angle $\Delta\Omega = 9.6$ msr and a momentum bite of 10% — was placed at 30.79°. This resulted in a central momentum transfer $q = 300$ MeV$/c$ and an energy transfer $\omega = 84$ MeV.

The neutron TOF detector had been used previously for precision measurements of the magnetic form factor of the neutron [11,12]. The detector consisted of five NE102A plastic scintillators, having frontal dimensions of 25×25 cm^2, each read out by a single photomultiplier tube (PMT). The first three detectors (ΔE_i, $i = 1, 2, 3$) were 1-mm thick and served to distinguish charged from neutral particles. These were followed by two 50-mm-thick detectors (E_1 and E_2). All five scintillators were inclined by 30° with respect to the vertical plane in order to optimize the timing resolution. Between the two thick scintillators, a 1-cm-thick iron plate was placed so that no protons, in coincidence with the electrons detected in the spectrometer, could reach E_2. In this way, the signal in E_2 is due exclusively to neutrons and was used to establish the losses of neutrons in E_1 resulting from pileup (noise) in the ΔE_i detectors. The neutron detector was positioned along the momentum-transfer vector, at $-58.9°$ with respect to the beam, and at a distance of 7.8 m from the target center, thus subtending a solid angle of 1.1 msr. The assembly was surrounded by a shield consisting of 5 cm of lead and 25 cm of concrete, except at the front. There, the detector was shielded by a 1-mm Pb plate which blocked low-energy background but was thin enough to allow the detection in E_1 of protons from the reaction ^{4}He$(e, e'p)^3$He. These events were used to calibrate the light response of the PMTs. In addition, a lead collimator of dimensions 10×1 cm^2 and thickness of 5 cm was placed in front of the 1-mm Pb sheet. This resulted in a limitation of the proton solid angle of the detector to 1/54 of the neutron one and reduced the data-acquisition dead time.

Neutrons and protons in the TOF detector were distinguished by their energy deposit in ΔE_i: the analog-to-digital converter (ADC) signal for protons was required to be above a certain (software) threshold value for all three ΔE_i, whereas the individual-detector signal for neutrons corresponded to the ADC-pedestal value which was slightly broadened due to pileup. Neutron events were identified by requiring that the ADC's of two of the three ΔE_i counters were below threshold [11,12].

The track reconstruction of the detected electrons yielded a position resolution of 1 mm along the beam line, which allowed the rejection of events originating from the target walls. Subsequently, cuts were applied to the time-of-flight of the electrons from the target to the spectrometer focal plane, and the timing walk was corrected. The setup accepted a range of nucleon energies, which led to broadening of the raw coincidence signal. Based on the electron kinematics, the kinetic energy of the quasielastically scattered nucleons was determined and used to correct the broadening. Finally, in the case of protons, corrections for energy losses from the target to the detector were considered. All these resulted in a corrected TOF spectrum [Fig. 1(a)] with a signal-to-noise ratio of 2.6.

The neutron missing-energy (E_m) spectrum is shown in Fig. 1(b). It was obtained by integrating over the entire acceptance of the experiment after subtraction of the time-uncorrelated background. Neutrons from the ^{4}He$(e, e'n)^3$He channel are centered in a peak at 20.5 MeV with a width of about 4 MeV. The contribution of the ^{4}He$(e, e'n)pd$ and ^{4}He$(e, e'n)ppn$ channels, which should show up at $E_m \geq 26$ MeV, appears to be negligible under the kinematical conditions of this experiment.

The experimental cross section is deduced from the neutron yield after several corrections have been applied (see [13] for a more comprehensive discussion):

Neutron detection efficiency.—The neutron-detection efficiency had been extensively studied and precisely measured in the past [11,12]. In the present experiment, this procedure began with the calibration of the ADC response that was accomplished via the ^{4}He$(e, e'p)^3$H reaction. Then, the detector response was simulated using

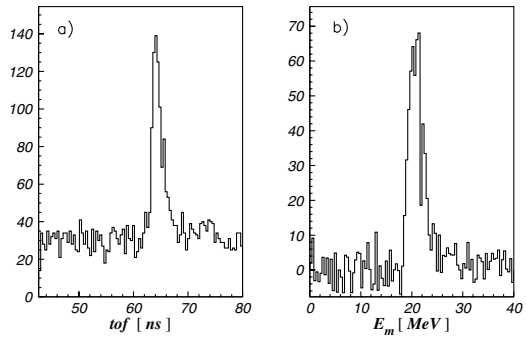

FIG. 1. (a) TOF spectrum for neutrons in E_1 after all corrections discussed in the text, and (b) missing-energy spectrum for the reaction ^{4}He$(e, e'n)^3$He after background subtraction.

the ENIGMA Monte Carlo code [14], with the uncertainty in these simulations proving to be negligible due to the small solid angle of the detector. The ENIGMA corrected neutron yield was found to be independent of the software ADC threshold, which establishes the validity of the efficiency correction. The relative uncertainty of this correction contained several contributions totalling 5.5% in quadrature.

Neutron losses.—These losses, which resulted from interactions in the ΔE_i detectors, were calculated by comparing the number of neutrons in the time-to-digital converter (TDC) peak of the E_2 spectrum with and without the veto condition. Within the 10% statistical uncertainty per bin (see below), the number of neutrons observed in the E_2 counter was the same for both cases, from which it was concluded that these losses were insignificant.

Proton misidentification.—A certain number of protons fall below the ΔE_i thresholds and, thus, are misidentified as neutrons. However, due to the long flight path, these protons show up in a separate missing-energy peak since corrections for energy losses are not applied for them. The contribution of these events to the neutron yield was determined to be less than 1%.

Neutron absorption.—Neutron absorption in the lead shield in front of the detector was simulated using ENIGMA [14] and GEANT [15] and found to be 5%.

Radiative corrections.—The data have been corrected for internal and external bremsstrahlung by folding standard radiative corrections [16] with the electron-detector acceptance. The corrections were $17.5\% \pm 0.5\%$ and $0.5\% \pm 0.1\%$, respectively, where the errors result from uncertainty in the energy and target-thickness calibration.

The experimental data in the acceptance range of 25–70 MeV/c were divided into three missing-momentum bins of equal width. Once all the aforementioned corrections were applied, the cross section for each bin was calculated by fitting the ground-state-transition peak in Fig. 1(b). The result proved to be insensitive to the precise fitting parameters. The fivefold differential cross sections are given in Table I, together with the statistical and the systematic uncertainties for each missing-momentum bin. The former has contributions from the experimental yield and the background-subtraction procedure and was found to be 11% for each p_m bin. An extensive study of the systematics [13] showed that they were dominated by the uncertainties in the neutron-detection efficiency and the accuracy of the target-thickness measurement. They are of the same order of magnitude as the statistical uncertainties and result essentially in a common normalization uncertainty.

TABLE I. Experimental differential cross sections.

Bin No.	p_m (MeV/c)	$d^5\sigma_{\mathrm{exp}}$	$\Delta d^5\sigma_{\mathrm{stat.}}$	$\Delta d^5\sigma_{\mathrm{syst.}}$
		$\times 10^{-6}(\mathrm{fm}^2\,\mathrm{MeV}^{-1}\,\mathrm{sr}^{-2})$		
1	25–40	2.10	±0.24	±0.17
2	40–55	1.55	±0.17	±0.13
3	55–70	1.16	±0.13	±0.10

Microscopic model calculations [17] of the ^{4}He$(e, e'n)$ reaction have been performed using an extension of the diagrammatic approach [18] which has already successfully been used for the ^{4}He$(e, e'p)$ reaction (see Ref. [2]). The reaction amplitudes are expanded in terms of the relevant diagrams, and the elementary current operators are reduced from their relativistic form into a nonrelativistic one, incorporating all the terms up to (and including) order $1/m^3$ in the nucleon mass. For the initial ^{4}He and final ^{3}He states, variational wave functions of the Urbana group [19] have been used that are projected onto the various spin-isospin states of NN pairs, while half-off-shell NN scattering amplitudes are used in the final state. This model comprises one- (PWIA) and two-body (MEC, FSI) reaction mechanisms. Particularly, as depicted in Fig. 2, FSI take into account all combinations for scattering between the struck nucleon and a second nucleon, with one of them being reabsorbed into the recoiling ^{3}He.

The comparison between the experimental cross section and the theoretical calculations, averaged over the detector acceptance, is presented in Fig. 3. The full calculation reproduces the magnitude of the ^{4}He$(e, e'n)^3$He cross section. PWIA alone underestimates the experimental cross section significantly, in qualitative agreement with the findings of Daman [4]. The global effect of the rescattering process is to add significant strength to the $(e, e'n)$ cross section. The rescattering is broken down into elastic rescattering (Resc.) of the knocked out neutron that contributes mildly, and into the charge-exchange process $(e, e'p)(p, n)$ (Exch.) (Fig. 2) that provides the bulk of the cross section. In the momentum range covered by the experiment, the neutron-rescattering amplitude is small compared to the quasielastic one, with which it interferes destructively. This is caused by a shift of strength from the quasielastic peak to higher recoil momenta [20]. On the contrary, the $(e, e'p)(p, n)$ charge-exchange amplitude is driven by the Coulomb part of the proton's electromagnetic current, which is strongly reduced in the quasielastic scattering of the electron off

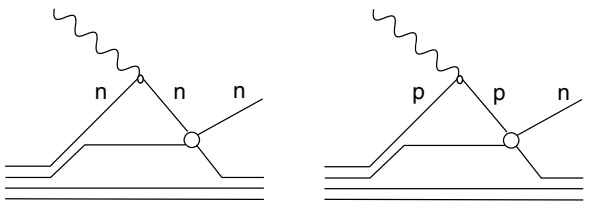

FIG. 2. The dominant FSI graph is broken down into elastic neutron rescattering (left) and charge-exchange proton rescattering (right).

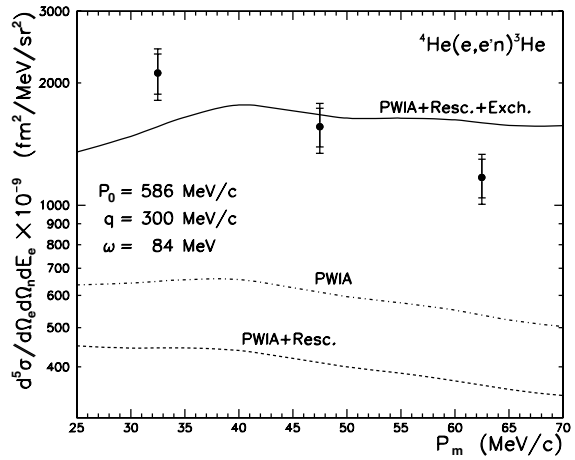

FIG. 3. The experimental cross section (dots) for the reaction ^{4}He$(e, e'n)^3$He compared to microscopic calculations [15]. The statistical and the quadratic combination of the statistical and systematical errors are shown.

the neutron. In these kinematics, the MEC contribution suppresses the cross section by only 1%.

Whereas the model is able to predict the magnitude of the ^{4}He$(e, e'n)^3$He cross section, it does not reproduce the slope of the momentum distribution. This may be due to the truncation of the multiple-scattering series to the first dominant term in the single scattering and beckons for a complete treatment of the 4-body final state.

In summary, the differential cross section of the ^{4}He$(e, e'n)^3$He reaction was measured with a statistical uncertainty of 11%, at a momentum transfer of 300 MeV$/c$ for small missing-momentum values. Final state interactions, specifically $(e, e'p)(p, n)$ charge exchange, are the main cause for the large enhancement of the ^{4}He$(e, e'n)^3$He cross section over PWIA. The main effect of FSI is the net channeling of $(e, e'p)$ strength into the $(e, e'n)$ reaction from the two-step process $(e, e'p)(p, n)$. The $(e, e'n)$ reaction turns out to be more sensitive than the $(e, e'p)$ channel to reaction mechanisms. Clearly, whereas the charge-exchange reaction shuffles strength between both QES channels, the effect is more pronounced in the electron-neutron reaction because of the much larger cross section of the primary electron-proton channel.

This experiment has provided unambiguous evidence of the different behavior of $(e, e'p)$ and $(e, e'n)$ QES and a unique example of the importance of the multistep processes in the small missing-momentum region. The lack of free neutron targets calls for further theoretical and experimental investigations of this channel. Clearly, our results are a strong warning against the simple-minded use of light nuclei as neutron targets in electrodisintegration experiments, without taking into account the implications of strong rescattering effects.

The authors thank A. van den Brink and the Utrecht mechanics team for their help during the experiment. This work was supported in part by the Stichting voor Fundamenteel Onderzoek der Materie (The Netherlands), the Natural Sciences and Engineering Research Council (Canada), NATO, and the Centre National de la Recherche Scientifique (France).

[1] J. J. Kelly, Adv. Nucl. Phys. **23**, 75 (1996).
[2] J. F. J. van den Brand *et al.*, Phys. Rev. Lett. **60**, 2006 (1988); **66**, 409 (1991).
[3] A. Magnon *et al.*, Phys. Lett. B **222**, 352 (1989).
[4] M. A. Daman, Ph.D. thesis, Universiteit van Amsterdam, 1991; H. P. Blok, Few-Body Syst., Suppl. **7**, 120 (1994).
[5] G. van der Steenhoven *et al.*, Phys. Lett. B **191**, 227 (1987).
[6] J.-E. Ducret *et al.*, Nucl. Phys. **A556**, 373 (1993).
[7] J.-M. Le Goff *et al.*, Phys. Rev. C **50**, 2278 (1994).
[8] J. J. van Leeuwe *et al.*, Phys. Rev. Lett. **80**, 2543 (1998).
[9] L. de Vries *et al.*, Nucl. Instrum. Methods Phys. Res., Sect. A **292**, 629 (1990).
[10] C. de Vries *et al.*, Nucl. Instrum. Methods **223**, 1 (1984).
[11] F. C. P. Joosse, Ph.D. thesis, Universiteit Utrecht, 1993; H. Anklin *et al.*, Phys. Lett. B **336**, 313 (1994).
[12] E. E. W. Bruins, Ph.D. thesis, Universiteit Utrecht, 1995; E. E. W. Bruins *et al.*, Phys. Rev. Lett. **75**, 21 (1995).
[13] A. Misiejuk, Ph.D. thesis, Universiteit Utrecht, 1997.
[14] J. L. Visschers, in *MC93 International Conference on Monte Carlo Simulations in High Energy and Nuclear Physics*, edited by P. Dragovitsch, S. L. Linn, and M. Burbank (World Scientific, Singapore, 1994), p. 350.
[15] R. Brun, F. Carminati, F. Bruyant, and M. Maire, CERN Computer Newsletter **200**, 13 (1990).
[16] L. W. Mo and Y. S. Tsai, Rev. Mod. Phys. **41**, 205 (1969).
[17] J.-M. Laget, Nucl. Phys. **A579**, 333 (1994).
[18] J.-M. Laget, in *New Vistas in Electronuclear Physics*, edited by E. L. Tomusiak, H. S. Caplan, and E. T. Dressler (Plenum, New York, 1986), p. 361.
[19] R. Schiavilla *et al.*, Nucl. Phys. **A449**, 219 (1986).
[20] J.-M. Laget, Phys. Rev. C **35**, 832 (1987), and references therein.